Biotechnology Reports 17 (2018) 16–23

Contents lists available at ScienceDirect

Biotechnology Reports

journal homepage: www.elsevier.com/locate/btre

Characterization of *Scenedesmus obtusiusculus* AT-UAM for high-energy molecules accumulation: deeper insight into biotechnological potential of strains of the same species

Alma Toledo-Cervantes[a,1], Gloria Garduño Solórzano[b], Jorge E. Campos[c], Martha Martínez-García[c], Marcia Morales[d,*]

[a] Doctorado en Ciencias Biológicas y de la Salud, Universidad Autónoma Metropolitana – Iztapalapa, Ciudad de México, Mexico
[b] Herbario IZTA, FES Iztacala, UNAM, Mexico
[c] Lab. Bioquímica Molecular, UBIPRO, FES Iztacala, UNAM, Mexico
[d] Departamento de Procesos y Tecnología, Universidad Autónoma Metropolitana-Cuajimalpa, Ciudad de México, Mexico

ARTICLE INFO

Keywords:
Carbohydrates
ITS2
Lipids
Morphological characterization
Scenedesmus obtusiusculus

ABSTRACT

Scenedesmus obtusiusculus AT-UAM, isolated from Cuatro Ciénegas wetlands in Mexico was taxonomically, molecularly and biochemically compared to *S. obtusiusculus* CCAP 276/25 (Culture Collection of Algae and Protozoa, Scotland, UK). Analysis of Internal Transcribed Spacer 2 (ITS2) secondary structures confirmed that the mexican strain belongs to *S. obtusiusculus* with one change in the ITS2 nucleotide sequence. However, both strains exhibited different biochemical and fatty acid profiles and therefore biotechnological potential, emphasizing the need for deeper studies among strains of the same species. Furthermore, the biochemical variations of *S. obtusiusculus* AT-UAM under nitrogen starvation and different levels of irradiance were evaluated. The maximum lipid production (1730 mg L^{-1}) was obtained at 613 µmol $m^{-2} s^{-1}$ while the highest carbohydrate content (49%) was achieved at 896 µmol $m^{-2} s^{-1}$. Additionally, this strain was capable of storing lipids (~52%) and carbohydrates (~40%) under outdoor condition depending on the light availability in the cultivation broth.

1. Introduction

Microalgae are important biological resources with a wide range of biotechnological applications. Some of them are green microalgae such as *Chlorella*, *Dunaliella* and *Scenedesmus*, the last belonging to Scenedesmaceae which currently include 43 recognized genera [1,2]. The *Scenedesmus* Meyen genus is pleomorphic and often overrated [3]. The main morphological characteristics to recognize *Scenedesmus* cells are the straight or slightly curved laminar coenobia in which the cells are generally arranged in one or two lines. Currently, the green microalgae classification is continuously relocating these *taxa*, since it only considers the morphological characteristics due to few molecular sequences available [4]. Likewise, *Scenedesmus* taxonomy does not include the cryptic species belonging to *taxon* in which only the nucleotide sequence differences can be observed, while morphology is indistinguishable. Although microalgae have been studied as source for biofuel and chemical production [5], little attention has been paid to the taxonomic issues of the involved species. In this context, Wynne and Hallan [6] have recently reinstated *Tetradesmus* genus. Hegewald et al. [1] characterized some *taxa* of Scenedesmaceae morphologically and molecularly, nevertheless, native *Scenedesmus* strains still need to be characterized.

The *S. obtusiusculus* AT-UAM strain was isolated from the wetlands of Cuatro Ciénegas, Mexico, located in the center of the Chihuahua desert valley [7]. This microalga was studied for its capacity to store lipids (up to 55.7%) and for the CO_2 tolerance (10% of CO_2 v/v). Furthermore, the optimal conditions for growth and lipid production under nitrogen starvation were recently determined by photosynthetic activity assays [8]. However, the biochemical composition of microalgae may vary as a result of different irradiance levels, photoacclimation and other environmental conditions. In photoacclimation processes, microalgae undergo dynamic changes in cell composition (ultrastructural, biophysical and physiological) in order to increase the rate of photosynthesis. Therefore, some authors have reported the increase in lipid and carbohydrate content and changes in the fatty acid profile at different irradiances [9]. In this context, understanding the effect of culture conditions, mainly irradiance, on the biochemical composition (lipids, carbohydrates and proteins) of microalgae may

* Corresponding author at: Universidad Autónoma Metropolitana-Cuajimalpa, Av. Vasco de Quiroga 4871, Colonia Santa Fe Cuajimalpa, México D.F., C.P. 05300, Mexico.
E-mail address: mmorales@correo.cua.uam.mx (M. Morales).
[1] Present address: Departamento de Ingeniería Química, CUCEI-Universidad de Guadalajara, Blvd. M. García Barragán 1451, C.P. 44430, Guadalajara, Jalisco, Mexico.

https://doi.org/10.1016/j.btre.2017.11.009
Received 7 October 2017; Received in revised form 11 November 2017; Accepted 30 November 2017
Available online 05 December 2017

lead to the development of suitable biofuel production processes, if the optimum conditions are applied.

This work aims to compare two strains of *S. obtusiusculus* by DNA (specifically the ITS region) and biochemical analysis considering the morphological similarity among Scenedesmus *sensu lato* and a presumed difference in their biofuel production potential. Moreover, the composition of carbohydrates, lipids and fatty acids of *S. obtusiusculus* AT-UAM at different irradiances under nitrogen starvation was evaluated in order to determine the best conditions for biofuel production.

2. Materials and methods

2.1. Taxonomic characterization of S. obtusiusculus strains

Scenedesmus obtusiusculus AT-UAM deposited at the IZTA herbarium (IZTA 1830) and *S. obtusiusculus* CCAP 276/25 (Culture Collection of Algae and Protozoa, Scotland, UK) were cultured in petri dishes with solid BG11 medium (10 gL^{-1} of Noble Agar, A5431 Sigma-Aldrich). BG11 medium composition was in $g\,L^{-1}$: $NaNO_3$, 1.5; K_2HPO_4, 0.04; $MgSO_4$ $7H_2O$, 0.075; magnesium disodium EDTA, 0.001; $CaCl_2$ $2H_2O$, 0.036; citric acid, 0.006; ferric ammonium citrate, 0.006; Na_2CO_3, 0.02; and the following salts in $mg\,L^{-1}$: H_3BO_3, 2.86; $MnCl_2$ $4H_2O$, 1.81; $ZnSO_4$ $7H_2O$, 0.222; $NaMoO_4$ $2H_2O$, 0.39; $CuSO_4$ $5H_2O$, 0.079; $Co(NO_3)_2$ $6H_2O$, 0.494.

Strains were grown at the same temperature (25 °C) and irradiance (96 $\mu mol\,m^{-2}\,s^{-1}$). The morphological identification of *S. obtusiusculus* AT-UAM was previously reported by Toledo-Cervantes et al. [7]. Electron microscopic analyses were done according to Del Castillo et al. [10], whereas scanning electron microscopic (SEM) and transmission electron microscopic (TEM) observations provided more detailed information about morphological features, size, shape and arrangement of organelles.

2.2. Molecular characterization of S. obtusiusculus strains

The genomic DNA of *S. obtusiusculus* AT-UAM and *S. obtusiusculus* CCAP 276/25 were extracted using the Ultran Clean Plant DNA Isolation kit (MoBio laboratories) according to the manufacturer's instructions. The 18S rDNA gene was amplified by polymerase chain reaction (PCR) using the forward SSU1 (5′TGG TTG ATC CTG CCA GTA-3′) and reverse SSU2 (5′TGA TCC TTC CGC AGG TTC AC-3′) primers. The ITS and ITS2 regions and 5.8S genes were amplified using the forward ITS 1800 (5′-ACC TGC GGA AGG ATC ATT G -3′) and reverse ITS4 (5′-TCC TCC GCT TAT TGA TAT GC-3′) primers. PCR products were sequenced in a 3130XL Applied Biosystem-Hitachi sequencer. The alignment of the respective 18S rRNA, 5.8S and ITS2 gene sequences and the analysis of similarity were completed with Basic Local Alignment Search Tool (BLAST) in the GenBank database of the National Center for Biotechnology Information. Phylogenetic tree based on ITS2 (248 bp) was constructed by Geneious program using the Jukes-Cantor model with 10,000 repetitions and the Neighbor-joining method. ITS sequence-structure analyses were carried out according to Schultz and Wolf [11] using the ITS2 Database (http://its2.bioapps.biozentrum.uni-wuerzburg.de). A BLAST search in the web interface of the ITS2 database was performed to identify sequence-structure pairs [12]. Global multiple sequence structure alignments were generated by remote 4SALE alignment which synchronously align the sequence and secondary structure using an ITS2-specific scoring matrix [13] and structure viewers as was implemented in 4SALE [14]. Finally, consensus ITS2 secondary structures were constructed using the Inkscape software (https://inkscape.org/es/).

2.3. Photobiorectors: inoculation and operation conditions

S. obtusiusculus AT-UAM and *S. obtusiusculus* CCAP 276/25 were individually cultured in 1 L bubbled columns (10 cm diameter and 20 cm height) supplying a 5% CO_2-air mixture at a flow rate of 1.5 $L\,min^{-1}$ through a stainless-steel diffuser placed at the bottom. The photobioreactors were autoclaved prior to inoculation and the CO_2-rich gas stream was filtered (0.22 μm pore size air filter) to avoid cross-contamination.

For the biochemical comparison of *Scenedesmus* strains, the photobioreactors were placed into a temperature control chamber (25 °C) with fluorescent light tubes providing an irradiance of 96 $\mu mol\,m^{-2}\,s^{-1}$. The reactors were inoculated with microalgae colonies obtained from petri dishes and operated during 8 days.

Indoor and outdoor experiments under nitrogen starvation were carried out by inoculating a specific microalgae culture volume of *S. obtusiusculus* AT-UAM according to the biomass concentration set (250, 500 and 1000 $mg\,L^{-1}$). The inoculum was pre-washed (centrifuged at 4000 rpm for 10 min and washed twice with distilled water) to ensure the absence of nitrogen in the cultivation broth. N-free 2x BG11 medium was used to guarantee no other nutrient limitation. For indoor cultivation, a cylindrical panel with LED lamps (5 m with 300 LEDs) was placed around the photobioreactors to regulate irradiance between 154 and 896 $\mu mol\,m^{-2}\,s^{-1}$. Temperature was controlled at 25 °C for the indoor experiments, while outdoor experiments were carried out with no temperature control and at solar irradiance. The artificial light and the solar irradiance were recorded with a light meter (Extech Instruments 407026sp model 2.2, USA).

2.4. Biochemical characterization of S. obtusiusculus strains

The biochemical comparison was carried out by culturing both strains in the bubbled columns as described before (See Section 2.3). After 8 days of cultivation, the biomass concentration was measured by dry weight. The biochemical profile was determined by spectrophotometric and fluorescent methods and the fatty acid methyl esters (FAMEs) profile by GC-FID analysis (see Section 2.6). At the end of the experimental period, the total biomass was recovered by centrifugation and oven-dried (60 °C) to determine the total lipid content by direct extraction with hexane and the inorganic fraction by incineration.

2.5. Effect of irradiance on the biochemical composition of S. obtusiusculus AT-UAM strain

The effect of irradiance was evaluated following two approaches: 1) At different initial biomass concentrations to study the effect of the self-shading that modifies the internal irradiance and, 2) at different levels of external irradiance; both were assayed under nitrogen starvation. Accordingly, *S. obtusiusculus* AT-UAM was cultivated indoor and outdoor as described in Table 1. The experiments were carried out in the photobioreactors described in Section 2.3. An aliquot of 5 mL was taken daily to quantify the biomass concentration and the biochemical composition by spectrophotometric methods. At the end of the experimental period, the composition of FAMEs, ashes and the total lipid content were determined asdescribed in Section 2.6.

Table 1
Initial biomass concentrations and irradiances evaluated during the experimentation.

Indoor conditions						
Initial biomass concentration ($mg\,L^{-1}$)			Artificial irradiance ($\mu mol\,m^{-2}s^{-1}$)			
250	500	1000	154	343	613	896
Outdoor conditions						
Initial biomass concentration ($mg\,L^{-1}$)			Solar irradiance ($\mu mol\,m^{-2}s^{-1}$)			
100	250	500	0–2064			

2.6. Analytical methods

Biomass concentration was determined at 665 nm by correlation with a reference curve constructed with optical density (OD) versus grams of algal biomass per liter. Carbohydrate content was determined by a modified phenol–sulfuric acid method [15]. A mixture of 5 mL of 1 M H_2SO_4 and 1 mL of cultivation broth was sonicated for 20 min. Afterwards, the sample was boiled for 20 min and centrifuged for 20 min at 4000 rpm. A volume of 0.5 mL of supernatant was mixed with 0.5 mL of a 5% phenol solution and allowed to rest for 40 min, 2.5 mL of concentrated H_2SO_4 were then added. The OD was read at 485 nm and compared to a D+ glucose calibration curve.

Protein content was measured by a modified Lowry method [16]. A mixture of 1 mL of NaOH 0.2 N and 1 mL of cultivation broth was boiled for 20 min and centrifuged for 20 min at 4000 rpm. The supernatant was analyzed by following the manufacture's protocol of the Bio-Rad protein assay kit. The OD was read at 750 nm and compared to a bovine serum albumin calibration curve. Chlorophyll was extracted with methanol (90%) and analyzed as described by Toledo-Cervantes [7].

Daily lipid content was determined by Nile red staining (N3013, Sigma Aldrich). A sample of 20 µL of cultivation broth was mixed with 100 µL of dimethyl sulfoxide and stirred for 1 min. The mixture was heated in a microwave oven (100% power 1650 W) for 50 s, 20 µL of Nile Red solution (0.25 mg L^{-1} in acetone) and 860 µL of distilled water were then added. The resulting mixture was stirred for another minute and heated again for 60 s and allowed to stand for 10 min in the dark. The total volume was then transferred to a 2 mL vial containing 1 mL of distilled water and analyzed in a fluorometer (Turner Designs Instrument model 7200-000, Sunnyvale CA, USA). Excitation and emission band on the equipment were set at 485 and 585 nm, respectively. Data (Reference Fluorescent Units, RFU) were compared to a calibration curve constructed as RFU versus grams of lipids obtained from microalgae by direct extraction with hexane (Soxhlet method) [7,8].

For total lipid analysis, the biomass was recovered by centrifugation and oven dried; afterwards, it was pulverized in a mortar, and sieved at 1 mm mesh. Hexane was used to extract the lipids for 8 h in Soxhlet extraction system at a drop rate of 4 drops per second. The lipid fraction was determined gravimetrically after nitrogen-drying of the extracted lipids. The FAMEs profile was determined by gas chromatography prior to acid derivatization using a mixture of 1 mL of dichloromethane and 2 mL of methanol/HCl (4:1 v/v) and heating at 110 °C for 6 h. A gas chromatograph (HP6890, Agilent Technologies) equipped with a flame ionization detector and a 30 m long capillary column (AT-FAME, No. 12436 Alltech) with an internal diameter of 0.25 mm and 0.25 µm film thickness was used. The injection volume was 2 µL with a split ratio of 100:1. Helium was used as carrier gas at a flow rate of 20 cm s^{-1}. The injector and detector temperatures were set at 250 °C while a gradient temperature program was set in the oven. The initial oven temperature was 140 °C for 5 min, then increased to 220 °C at a rate of 5 °C min^{-1} and held for 4 min then increased from 220 to 240 °C at a rate of 2 °C min^{-1}, and finally held for 5 min at 240 °C. A mixture of 37 FAMEs at a concentration of 10 mg mL^{-1} in dichloromethane was used as standard (Supelco, Catalog No. 18919-1AMP). The inorganic content in the dried-biomass (ashes) was determined gravimetrically after incineration at 490 °C for 6 h.

3. Results and discussion

3.1. Taxonomic and molecular characterization of Scenedesmus obtusiusculus strains

The taxonomic characteristics of both strains exhibited similar features to those reported by Chodat [17] and Toledo-Cervantes et al. [7] (Table S1, Supplementary materials).

Microalgae included in the genus *Scenedesmus* Meyen have been recurrently reclassified into diverse subgenera over the years (See Supplementary materials for a brief history). In this context, taxonomic issues of *Scenedesmaceae* have been successfully solved by studying the nuclear regions 18S rDNA, 26S rDNA [18], ITS2 [19–21] and the combined information of 18S and 26S chloroplast genes–*atp*B. Nonetheless, debate over classification of several *taxa* continues. *Acutodesmus* has been recently transferred to *Tetradesmus* due to its priority over *Acutodesmus* (E. Hegewald) P. M. Tsarenko [6].

In this study, analysis of the 18S rDNA sequence of *S. obtusiusculus* AT-UAM (GenBank accession no. KJ808697.1) was compared with the data available in GebBank. However, there were no sequences for *S. obtusiusculus* strains found and data were not enough to unambiguously separate the related species, finding 99% similarity to *Tetradesmus incrassatulus* CCAP 276/43 by analyzing 1677 bp.

Detailed analysis of the ITS region of the closest species (i.e. *Tetradesmus incrassatulus* CCAP 276/43) and the acquired *S. obtusiusculus* CCAP 276/25 strain was then performed to determine the phylogenetic relation among the *Scenedesmus* species. The sequences obtained from the 5.8S partial sequence, ITS2 complete sequence and 28S rDNA partial sequence of *S. obtusiusculus* AT-UAM, *S. obtusiusculus* CCAP 276/25 and *T. incrassatulus* CCAP 276/43 were aligned. Fig. 1 shows the phylogenetic tree based on ITS2 rDNA sequences of the *Scenedesmus* species constructed with 248 bp. The *S. obtusiusculus* AT-UAM (GenBank accession no. KJ808697.1) and *S. obtusiusculus* CCAP 276/25 (GenBank accession no. KP318981.1) were located in the same clade, independent of *T. incrassatulus* CCAP 276/43 (GenBank accession no. FR865722).

The analysis of the ITS2 sequences and the secondary structure showed a typical characteristic of eukaryotes: four helices, being the third the largest and containing the UGG and GGU motifs (Fig. 2). Moreover, five changes in the alignment of the sequences were detected: 1) in the position 243, 2) in helix I position 31, 3) in helix II position 57, 4) in helix II position 111, and 5) in helix III position 145. The latest change corresponds to *S. obtusiusculus* AT-UAM in which the nucleotide G* modified the canonical interaction A-U of the secondary structure.

The analyzed *taxa* showed twice the G•U interaction in helix I, 9 times in helix II and 8 times in helix III. Furthermore, among nucleotides 51 and 111 a canonical interaction between A and T was established (helix II). Conversely, *T. incrassatulus* CCAP 276/43 did not present the interaction whereby in position 111 the nucleotide U was replaced by A and, consequently, the helix structure was modified. Positions 57 and 96 belonging to *T. incrassatulus* CCAP 276/43 also produced an internal buckle while *S. obtusiusculus*, *T. naegelii* and *T. obliquus* kept a G•U interaction. At this point, it must be highlighted that *S. obtusiuculus* AT-UAM showed a base pairing G•U in positions 145 and 186 of helix III while the sequences of the analyzed *taxa* presented a canonical pairing A•U. These results confirmed the phylogenetic tree topology (Fig. 1) and remarked the structural differences between the *T. incrassatulus* CCAP 276/43, *S. obtusiusculus* CCAP 276/25 and *S. obtusiusculus* AT-UAM.

3.2. Biochemical composition of S. obtusiusculus strains

Despite the taxonomic similarities, the molecular difference of both strains was supported by different biochemical and fatty acid profiles depicted in Table 2. *S. obtusiusculus* CCAP 276/25 stored a high amount of carbohydrates (~43%), which was corroborated by TEM observation as white starch granules (Table S1, Supplementary materials). In contrast, *S. obtusiusculus* AT-UAM showed a high content of proteins (~51%) related to the low content of carbohydrates (~18%) and lipids (~19%).

Although the global lipid content was similar in both strains, the fatty acid composition was different. The FAMEs composition of *S. obtusiusculus* AT-UAM was in the range of C16 to C18, which might have commercial applications (Table 2). For instance, palmitic acid

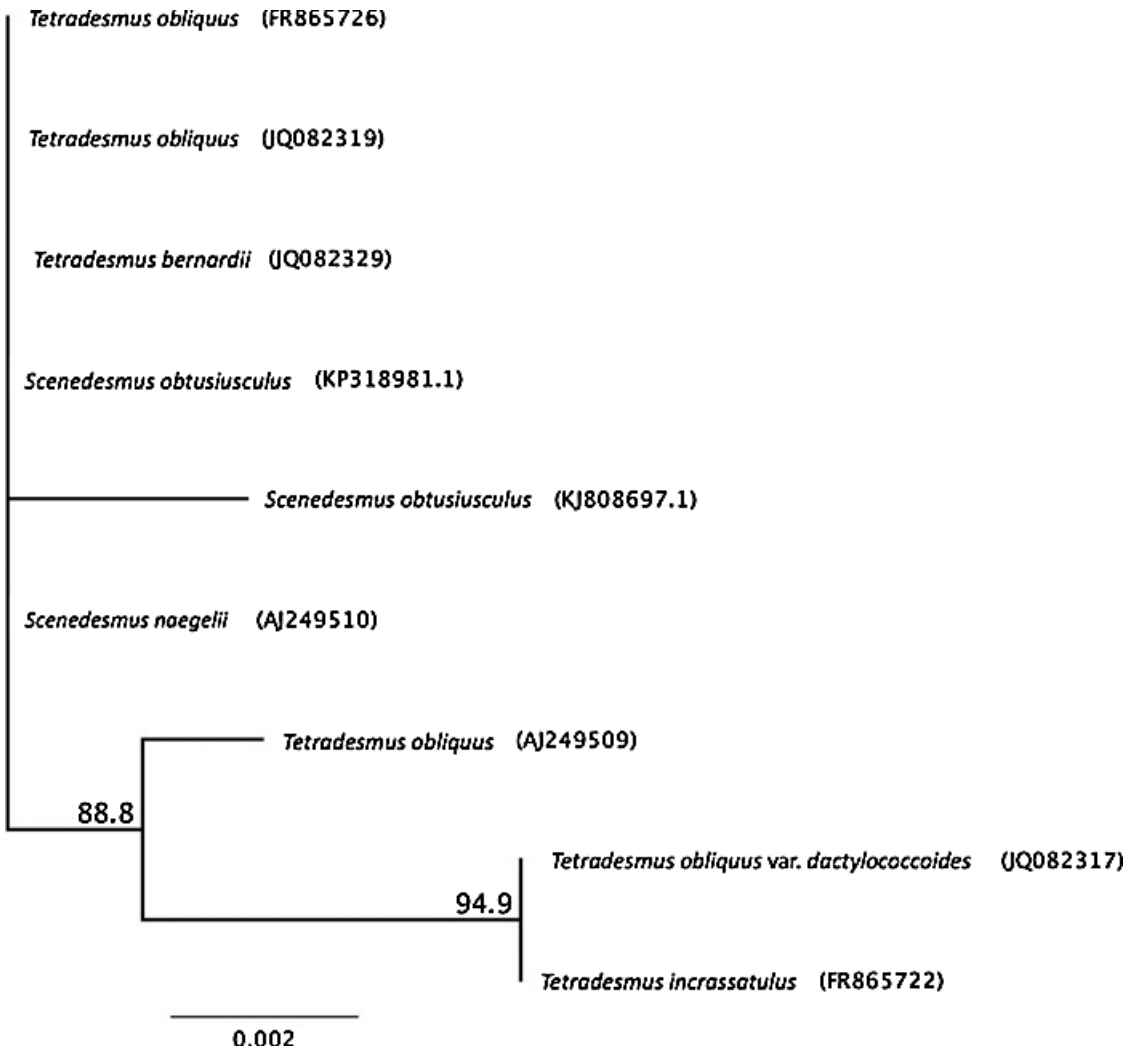

Fig. 1. Phylogenetic tree based on ITS2 rDNA sequences of some *Scenedesmus* species.

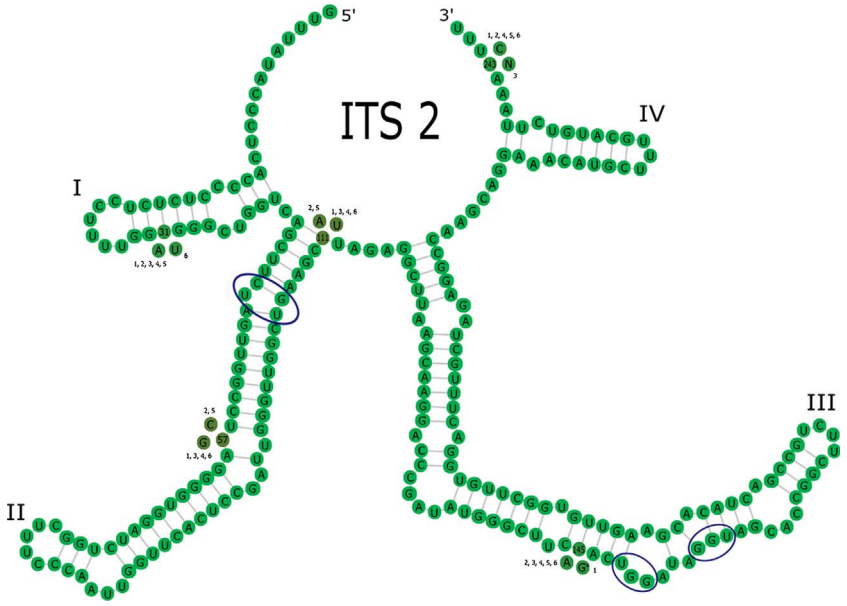

Fig. 2. Consensus ITS2 secondary structure model for: 1. *S. obtusiusculus* AT-UAM, KJ808697.1, 2. *T. incrassatulus* RF865722, 3. *T. naegelii* AJ249510, 4. *S. obtusiusculus* KP318981.1, 5. *T. incrassatulus* KP318982.1, 6. *T. obliquus* AJ249509, visualized with 4SALE [14,13]. Helices are numbered I–IV. Typical ITS2 motifs: a U–U mismatch in helix II and UGGU-motif 5′to the apex of helix III in circles. The number written inside the nucleotide indicates its position; G*belongs to *S. obtusiusculus* AT-UAM.

Table 2
Biochemical and fatty acid profiles of the *S. obtusiusculus* strains under nitrogen replete conditions. The data show the average values of the extractions performed in triplicate, at the end of growth (8 days). NF stands for not found.

Biochemical profile	*S. obtusiusculus* CCAP 276/25	*S. obtusiusculus* AT-UAM
Carbohydrates (%)	43.2 ± 3.5	18.3 ± 2.1
Lipids (%)	16.8 ± 2.3	19.2 ± 3.5
Proteins (%)	35.8 ± 1.5	51.3 ± 1.8
Chlorophyll (%)	1.5 ± 0.4	3.0 ± 0.7
Ash content (%)	2.7 ± 0.3	8.2 ± 1.1
Organic carbon content (%)	97.3 ± 0.6	91.8 ± 0.4
Palmitic acid. 16:0 (%)	25.6 ± 1.4	34.5 ± 1.2
Palmitoleic acid. C16:1 (%)	NF	4.1 ± 0.4
Oleic acid. C18:1n9c (%)	12.7 ± 0.5	21.9 ± 1.3
Elaidic acid. C18:1n9t (%)	NF	22.2 ± 1.1
Linoleic acid. C18:2n6c (%)	16.2 ± 0.7	NF
γ-linolenic acid. C18:3n6 (%)	NF	11.3 ± 0.4
Cis-11-Eicosenoic acid. C20:1 (%)	12.0 ± 0.9	NF
Arachidonic acid. C20:4n6 (%)	19.6 ± 1.1	NF
Others (%)	13.9 ± 0.5	6.0 ± 0.3

(C16: 0) is preferred in the production of biofuels (biodiesel) and cosmetics; palmitoleic acid is applied in skin care products; oleic acid is a food supplement, drug excipient, emulsifier and solubilizer in aerosols [22] and the γ-linolenic acid (C18: 3n6) is an omega 6 fatty acid. In contrast, the fatty acid profile of *S. obtusiusculus* CCAP 276/25 had long-chain polyunsaturated fatty acids (C16 to C23) such as omega 3 and 6 that are used as lubricants (C20: 1), feedstock for soaps, emulsifiers, beauty products and anti-inflammatory agents (C18: 2n6c). These results were not in agreement with the typical FAMEs composition reported for green algae in which only chain lengths in the range of C16 to C18 are expected, whereas long-chain fatty acids (> C20) are typically found in diatoms [23] and red algae [24]. However, some researchers have reported small quantities of fatty acids such as C20:0, C20:4. C23:0, C24:0 for *Chlorella* PY-ZU1 (a mutated strain) [25] and C20:0, C20:1n11, C20:5n3. C22:0, C22:1n9, C24:0 for *Scenedesmus rubescens* [26] when cultured under normal nutrition and combining nitrogen–phosphate deprived conditions, respectively. Higher concentration of C20:0 (Arachidic acid) around 7% was also reported for *Chlorella* sp., BUM11008 cultured under normal conditions and increased to 17% under N-deprived and up to 23% under N, K, P and Fe combination-deprived cultivation. Lignoceric acid (C:24) was also detected in a concentration of 27% of the total fatty acid composition under normal culture conditions and varying in the range of 0.7-30% under the different element-deprivation culture conditions [27]; however, no discussion about its presence was exposed. Therefore, the FAMEs composition of *S. obtusiusculus* CCAP 276/25 here reported, despite being unusual, might be the result of the macromolecular differences recorded, i.e. a single change in the ITS2 nucleotide sequence when compared to *Scenedesmus obtusiusculus* AT-UAM.

The FAMEs composition of microalgae oil and the carbohydrate content are often used to evaluate the capacity of algae for biofuels production. However, the differences, here observed, allow concluding that no extrapolation of the biotechnological potential of microalgae should be done, since even strains of the same species can present different FAMEs profile when cultured under the same conditions.

3.3. Effect of irradiance on the biochemical composition of *S. obtusiusculus* AT-UAM under indoor and outdoor conditions

In order to explore the biotechnological potential of the native *S. obtusiusculus* strain, an exhaustive analysis of its capacity for producing carbohydrates and lipids was performed by culturing it under nitrogen starvation and different irradiances (154–896 $\mu mol\, m^{-2}\, s^{-1}$).

S. obtusiusculus AT-UAM was able to store both carbohydrates and lipids under nitrogen starvation while decreasing its protein content at all irradiances tested (Fig. S1, Supplementary materials). The accumulation of lipids and carbohydrates was observed during days 4 to 8 of cultivation (Fig. S2, Supplementary materials). Klok et al. [28] have observed the accumulation of metabolites during the first hour or day after the culture was exposed to nitrogen starvation. A decrease in lipid accumulation rate was also observed after day 8. In this sense, there is a harvesting time for the target metabolite being the amount of a high-value metabolite (e.g. grams of lipids or carbohydrates per liter of cultured broth) a function of the biomass concentration and the percentage contained in the cells.

At an initial biomass concentration of 250 $mg\, L^{-1}$, the final biomass concentration (X) of the cultures was ~1000 $mg_B\, L^{-1}$ regardless of the irradiation supplied (Table 3). The increase in biomass concentration during nitrogen starvation has been observed on different microalgae species reaching up to 1.4–7.8 times the initial biomass concentration [29,30]. Regarding to lipid storing, at an initial biomass concentration of 250 $mg\, L^{-1}$ the maximum accumulation (55%) was obtained at 154 $\mu mol\, m^{-2}\, s^{-1}$ with a lipid productivity (P_L) of 110 ± 20 $mg_L\, L^{-1}\, d^{-1}$, and a maximum lipid content (Y) of 500 ± 10 $mg_L\, L^{-1}$ (Table 3). In contrast, the maximum percentage of carbohydrates (49%) was observed at 896 $\mu mol\, m^{-2}\, s^{-1}$ showing a carbohydrate productivity (P_{CH}) of 280 ± 20 $mg_{CH}\, L^{-1} d^{-1}$ (Table 3). The lipid fraction under this condition was mainly composed of oleic, palmitic and pentadecanoic acids (Table S2, Supplementary materials),

Table 3
Lipid productivities, carbohydrates productivities, lipid content and final biomass concentrations obtained at different light intensities and initial biomass concentrations. ND stands for not determined.

I ($\mu mol\, m^{-2}\, s^{-1}$)			154	343	613	896
Initial biomass concentration ($mg\, L^{-1}$)	250	P_L ($mg_L\, L^{-1}\, d^{-1}$)	110 ± 20	100 ± 20	66 ± 10	062 ± 30
		Y ($mg_L\, L^{-1}$)	500 ± 10	390 ± 13	170 ± 20	350 ± 11
		P_{CH} ($mg_{CH}\, L^{-1}\, d^{-1}$)	81 ± 10	100 ± 30	130 ± 10	280 ± 20
		X ($mg_B\, L^{-1}$)	1004 ± 47	1140 ± 23	976 ± 31	978 ± 25
	500	P_L ($mg_L\, L^{-1}\, d^{-1}$)	82 ± 20	200 ± 10	30 ± 10	27 ± 10
		Y ($mg_L\, L^{-1}$)	540 ± 20	620 ± 34	250 ± 20	230 ± 11
		P_{CH} ($mg_{CH}\, L^{-1}\, d^{-1}$)	91 ± 10	160 ± 10	170 ± 10	140 ± 30
		X ($mg_B\, L^{-1}$)	860 ± 20	1030 ± 34	766 ± 52	627 ± 11
	1000	P_L ($mg_L\, L^{-1}\, d^{-1}$)	170 ± 20	210 ± 10	240 ± 10	ND
		Y ($mg_L\, L^{-1}$)	1060 ± 100	1470 ± 130	1730 ± 110	ND
		P_{CH} ($mg_{CH}\, L^{-1}\, d^{-1}$)	200 ± 10	370 ± 20	390 ± 20	ND
		X ($mg_B\, L^{-1}$)	3127 ± 10	2960 ± 30	3446 ± 26	1076 ± 32

P_L = lipid productivity; Y = lipid content; P_{CH} = carbohydrate productivity; X = final biomass concentration. Lipid productivity, P_L, [$mg_L\, L^{-1}\, d^{-1}$] = P [$mg_B\, L^{-1}\, d^{-1}$] * Lipid content [$mg_L\, mg_B^{-1}$]. Lipid content, Y, [$mg_L\, L^{-1}$] = X [$mg_B\, L^{-1}$] * Lipid content [$mg_L\, mg_B^{-1}$]. Carbohydrate productivity, P_{CH}, [$mg_{CH}\, L^{-1}\, d^{-1}$] = P [$mg_B\, L^{-1}\, d^{-1}$] * carbohydrate content [$mg_{CH}\, mg_B^{-1}$]. Biomass productivity, P, [$mg_B\, L^{-1}\, d^{-1}$] = X − Xo/t- to. The subscript o corresponds to the initial time.

out of which 55% corresponded to palmitic acid under an irradiance of 613 μmol $m^{-2} s^{-1}$.

At 500 mg L^{-1} of initial biomass concentration, the maximum lipid accumulation and productivity (620 ± 34 $mg_L L^{-1}$ and 200 ± 10 $mg_L L^{-1} d^{-1}$, respectively) were obtained at 343 μmol $m^{-2} s^{-1}$. In addition, an increase in the carbohydrate content up to 32% was observed when irradiance increased from 154 μmol $m^{-2} s^{-1}$ to 343 μmol $m^{-2} s^{-1}$. These results were in agreement with that reported by Breuer et al. [31], where low incident light intensity was most beneficial for triacylglycerol production. Similarly, no significant effect over the lipid content of *S. obliquus* CNW-N by the impinging irradiance was observed [9]. Thus, the correlation between irradiance and lipid content is usually species-specific [32]. Similar to what has been observed at 250 mg L^{-1} of initial biomass concentration, 54% of the lipid fraction was palmitic acid under an irradiance of 613 μmol $m^{-2} s^{-1}$.

At 1000 mg L^{-1} of initial biomass concentration, the biomass was triplicated (Table 3) at the end of the experimental period except for the culture at 896 μmol $m^{-2} s^{-1}$. Therefore, no productivities were reported for 1000 mg L^{-1} due to the "crash" of the culture. This might be because of the combined effect of self-shading and high temperature observed (32 °C), since the optimum temperature and irradiance for *S. obtusiusculus* AT-UAM cultured under nitrogen starvation conditions are 28.5 °C and 100–200 μmol $m^{-2} s^{-1}$, respectively [8]. The maximum lipid productivity (240 ± 10 $mg_L L^{-1} d^{-1}$) and lipid content (1730 ± 110 $mg_L L^{-1}$) were observed at 613 μmol $m^{-2} s^{-1}$. The maximum lipid productivity, here observed, was lower than that reported by Cabello et al. [8], who reported that *S. obtusiusculus* AT-UAM is capable of storing 340 $mg_L L^{-1} d^{-1}$. However, this value highly depends on the photobioreactor configuration (flat panel reactor), the optimum operating parameters applied (28.5 °C, pH of 5.5 and of 100 μmol $m^{-2} s^{-1}$) and the lack of self-shading effect.

Table 3 shows the lipid content and lipid and carbohydrate productivities obtained at all biomass concentrations and irradiances tested. As can be seen, the lipid productivities of *S. obtusiusculus* AT-UAM were higher than the values reported for species such as: *S. obliquus* CNW-N, 140 $mg_L L^{-1} d^{-1}$ [9]; *Chlorella. vulgaris* ESP-31, 144 $mg_L L^{-1} d^{-1}$ [33]; *Nannochloropsis oculata*, 170 $mg_L L^{-1} d^{-1}$ [34], and *Scenedesmus* spp. 7–109 $mg_L L^{-1} d^{-1}$ [35]. Similarly, carbohydrate productivities were higher than those reported for species such as: *C. vulgaris* CCAP 211/11B, 21 $mg_{CH} L^{-1} d^{-1}$; *C. vulgaris,* 112 $mg_{CH} L^{-1} d^{-1}$; *S. obliquus* CNW-N, 383 $mg_{CH} L^{-1} d^{-1}$; *Chlamydomonas reinhardtii* UTEX 90, 304 $mg_{CH} L^{-1} d^{-1}$, and *C. reinhardtii*, 257 $mg_{CH} L^{-1} d^{-1}$ [36]. Thus, *S. obtusiusculus* AT-UAM has a biotechnological potential for the production of biofuels, such as bioethanol, biodiesel, biogas or the so-called "drop in biofuels".

The results here presented, showed that at higher initial biomass concentrations, a lower percentage of lipids was accumulated at an irradiance of 154 μmol $m^{-2} s^{-1}$. In contrast, an inverse behavior was observed at irradiances between 343 and 613 μmol $m^{-2} s^{-1}$. This might be caused by the self-shading effect where dense cultures are protected against high irradiance, which might damage the photosynthetic apparatus. In this context, Münkel et al. [30] have observed that the specific light availability, described as the impinging light to biomass concentration ratio (mol photons per gram of biomass) in a defined time interval, directly affects the lipid storage. In contrast, other authors have reported that irradiance has no effect on the content of carbohydrates, lipids and proteins, only on the chlorophyll content [37]. In this study, the irradiance effect was mainly observed through the decrease in intracellular nitrogen sources (proteins and chlorophylls) and the production of carotenoids. After two days of cultivation at all irradiances and initial biomass concentrations tested, the chlorophyll content was below the detection limit. Even though the excess of irradiance can cause damage in the photosystems, microalgae are able to resist and repair the photosystem II, as well as to reduce the oxidative stress by releasing heat [38,39].

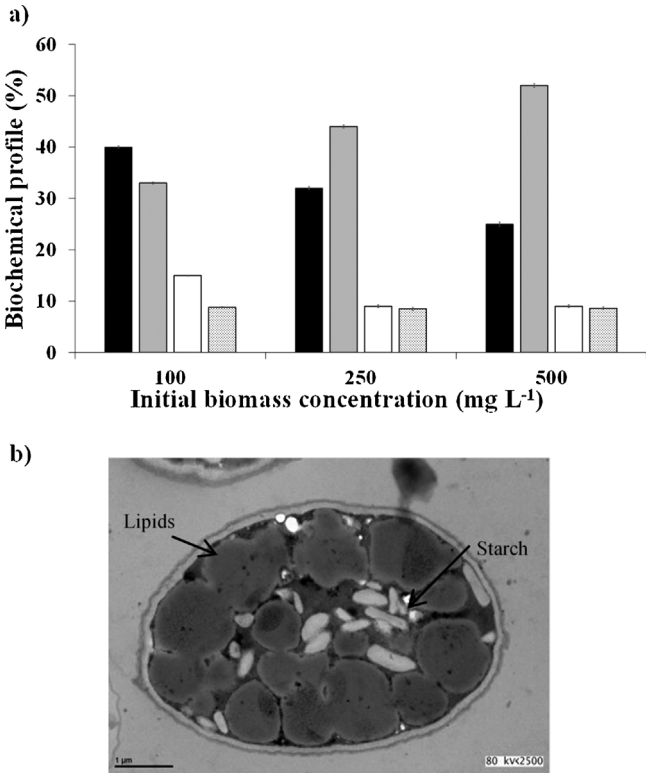

Fig. 3. a) Biochemical profile of *S. obtusiusculus* AT-UAM when cultured under outdoor conditions, black bars represent carbohydrates, gray bars lipids, white bars proteins and dotted bars the ash content. b) TEM cell micrograph of *S. obtusiusculus* AT-UAM showing high lipid content (gray globules) when cultivated under nitrogen starvation.

The results obtained under outdoor conditions were consistent with those observed at indoors (Figs. 3 and 4). The maximum accumulation of carbohydrates (40%) was obtained at an initial biomass concentration of 100 mg L^{-1}, which corroborates the induction of this metabolite at a higher light availability per cell. The final biomass concentration under this condition was 300 ± 25 $mg_B L^{-1}$ having a lipid productivity of 110 ± 18 $mg_L L^{-1} d^{-1}$ and a lipid content of 440 ± 35 $mg_L L^{-1}$. The maximum accumulation of lipids (52%) was obtained at 500 mg L^{-1} of initial biomass concentration. The final biomass concentration obtained was 1010 ± 42 $mg_B L^{-1}$ with a lipid content of 620 $mg_L L^{-1}$. At this point, it must be highlighted regarding the FAMEs profile, up to date, there are not conclusive results about the effect of irradiance on lipid accumulation in microalgae; some authors have reported slight [40,41] or high increase [42] in lipid content or change in the fatty acid profile [43]. *S. obtusiusculus* AT-UAM showed a composition of fatty acids relatively constant when cultured indoor at the best conditions (1000 mg L^{-1} of initial biomass concentration and 613 μmol $m^{-2} s^{-1}$) and outdoor conditions with > 75% of palmitic and oleic fatty acids (Fig. 4).

Results allow establishing that *S. obtusiusculus* AT-UAM strain was able to grow under uncontrolled conditions such as temperatures between 13 and 35 °C and irradiance up to 2064 μmol $m^{-2} s^{-1}$ without affecting the lipid/carbohydrate production performance. However, from a biofuel production point of view, if a continuous culture of *S. obtusiusculus* AT-UAM is intended for carbohydrate production, a biomass concentration of ~300 mg L^{-1} must be kept, while for lipid production it should be ~1000 mg L^{-1}, provided that irradiance typical of tropic is available.

4. Conclusions

The specific identity of the *S. obtusiusculus* AT-UAM strain was confirmed by morphological and molecular analyses showing the

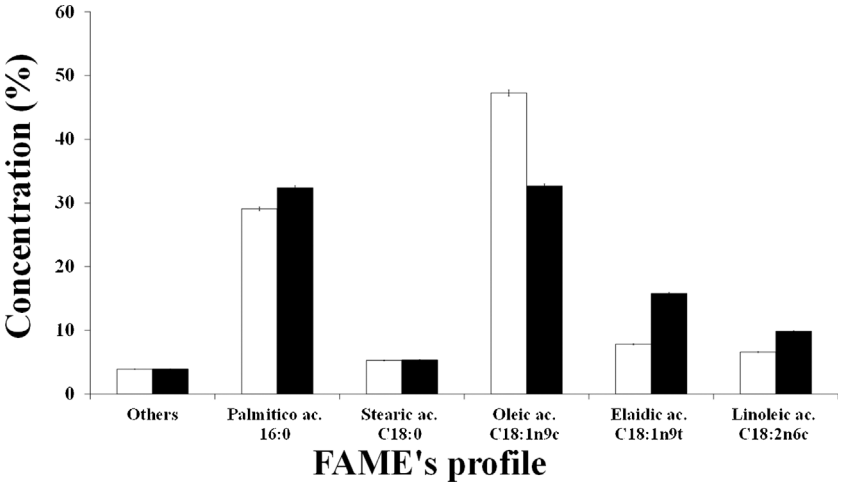

Fig. 4. Fatty acid methyl esters composition of *S. obtusiusculus* AT-UAM obtained under nitrogen starvation. White bars represent indoor cultivation at 613 μmol $m^{-2} s^{-1}$ and black bars outdoor culture.

relationship and differences with *S. obtusiusculus* CCAP 276/25. The different biochemical composition of both strains emphasized that the biofuel production potential of microalgae is not only species-specific but also strain-specific. The biochemical composition of *S. obtusiusculus* AT-UAM showed its potential to produce carbohydrates or lipids depending on the light availability in the cultivation broth with maximum lipid and carbohydrate accumulations of ~50%. In addition, outdoor experiments showed the robustness of this strain for storing high-energy molecules.

Conflict of interest

None.

Acknowledgments

CONACyT-México is gratefully acknowledged for the doctoral grant of Alma Toledo, grant 237873 and the financial support of the research projects SENER-CONACYT 247006 and PN-247402.

Appendix A. Supplementary data

Supplementary data associated with this article can be found, in the online version, at https://doi.org/10.1016/j.btre.2017.11.009.

References

[1] E. Hegewald, M. Wolf, A. Keller, T. Friedl, L. Krienitz, ITS2 sequence-structure phylogeny in the Scenedesmaceae with special reference to *Coelastrum* (Chlorophyta, Chlorophyceae), including the new genera *Comasiella* and *Pectinodesmus*, Phycologia 49 (2010) 325–335.
[2] M.D. Guiry, G.M. Guiry, AlgaBase. World-wide Electronic Publication, National University of Ireland, Galway, 2016 Available at: http://www.algaebase.org . (Accessed March 2016).
[3] S. Kaur, M. Sarkar, R.B. Srivastava, H.K. Gogoi, M.C. Kalita, Fatty acid profiling and molecular characterization of some freshwater microalgae from India with potential for biodiesel production, New Biotechnol. 29 (3) (2012) 332–344.
[4] F. Leliaert, D.R. Smith, H. Morearu, M.D. Herron, H. Verbruggen, C.F. Delwiche, O. de Clerck, Phylogeny and molecular evolution of the green algae, Crit. Rev. Plant Sci. 31 (2012) 1–46.
[5] N.K. Singh, D.W. Dhar, Microalgae as second generation biofuel. A review, Agron. Sust. Dev. 31 (2010) 605–629.
[6] M.J. Wynne, J.K. Hallan, Reinstatement of *Tetradesmus* G M. Smith (Sphaeropleales, Chlorophyta), Feddes Repertorium 126 (2016) 83–86.
[7] A. Toledo-Cervantes, M. Morales, E. Novelo, S. Revah, Carbon dioxide fixation and lipid storage by *Scenedesmus obtusiusculus*, Bioresour. Technol. 130 (2013) 652–658.
[8] J. Cabello, A. Toledo-Cervantes, L. Sánchez, S. Revah, M. Morales, Effect of the temperature, pH and irradiance on the photosynthetic activity by *Scenedesmus obtusiusculus* under nitrogen replete and deplete condition, Bioresour. Technol. 181 (2015) 128–135.
[9] S.H. Ho, C.Y. Chen, J.S. Chang, Effect of light intensity and nitrogen starvation on CO_2 fixation and lipid/carbohydrate production of an indigenous microalga *Scenedesmus obliquus* CNW-N, Bioresour. Technol. 11 (2012) 244–252.
[10] M.E.M. Del Castillo, M.E. Zamudio-Resendiz, L.F. Fernandes, *Fryxelliella sepulvedana* sp nov. (Triceratiaceae, Bacillariophyta), a rare species from the Mexican Pacific coasts. Iheringia, Série Botànica 63 (2008) 177–185.
[11] J. Schultz, M. Wolf, ITS2 Sequence-structure analysis in phylogenetics: a how-to manual for molecular systematics, Mol. Phylogenet. Evol. 52 (2) (2009) 520–523.
[12] C. Koetschan, T. Hacki, T. Müler, M. Wolf, F. Förster, J. Schultz, ITS2 database IV: interactive taxon sampling for internal trascribed spacer 2 based phylogenies, Mol. Phylogenet. Evol. 63 (3) (2012) 585–588.
[13] P.N. Seibel, T. Müller, T. Dandekar, M. Wolf, Synchronous visual analysis and editing of RNA sequence and secondary structure alignments using 4SALE, BMC Res. Notes 1 (2008) 91.
[14] P.N. Seibel, T. Müller, T. Dandekar, J. Shultz, M. Wolf, 4SALE–a tool for synchronous RNA sequence and secondary structure alignment and editing, BMC Bioinf. 7S (2006) 498.
[15] M. Dubois, K. Gilles, J. Hamilton, P. Rebers, F. Smith, Colorimetric method for determination of sugar and related substances, Anal. Chem. 28 (1956) 350–356.
[16] O. Lowry, N. Rosenbrough, A. Farr, R. Randall, Protein measurement with the Folin phenol reagent, J. Biol. Chem. 193 (1951) 265–272.
[17] R. Chodat, Monographies d'algues en culture pure, Materiaux pour la flore cryptogamique Suisse, (1913).
[18] M.A. Buchheim, E.A. Michalopulos, J.A. Buchheim, Phylogeny of the Chlorophyceae with special reference to the Sphaeropleales: a study of 18S and 26 rDNA data, J. Phycol. 37 (2001) 819–835.
[19] S.S. An, T. Fried, E. Hegewald, Phylogenetic relationships of *Scenedesmus* and scenedesmus-like coccoid green algae as inferred from ITS-2 rDNA sequence comparisons, Plant Biol. 1 (1999) 418–428.
[20] E.J. Van Hannen, M. Lürling, E. Van Donk, Sequence analysis of the ITS-2 region: a tool to identify strains of *Scenedesmus* (Chlorophyceae), J. Phycol. 36 (2000) 605–607.
[21] O. Kilian, P.G. Kroth, Molecular biology and genetic engineering in microalgae, in: D.V. Subba (Ed.), Algal Cultures Analogues of Blooms and Applications, vol. 2, Science publishers, USA, 2006, pp. 769–799.
[22] D.M. Prathima, Y.V. Swamy, M.S. Venkata, Nutritional mode influences lipid accumulation in microalgae with the function of carbon sequestration and nutrient supplementation, Bioresour. Technol. 142 (2013) 278–286.
[23] R. Moreno, G.M. Aita, L. Madsen, D.L. Gutierrez, S. Yao, B. Hurlburt, S. Brashear, Identification of naturally isolated Southern Louisiana's algal strains and the effect of higher CO_2 content on fatty acid profiles for biodiesel production, J. Chem. Technol. Biotechnol. 88 (5) (2013) 948–957.
[24] G. Su, K. Jiao, Z. Li, X. Guo, J. Chang, T. Ndikubwimana, Y. Sun, X. Zeng, Y. Lu, L. Lin, Phosphate limitation promotes unsaturated fatty acids and arachidonic acid biosynthesis by microalgae *Porphyridium purpureum*, Bioprocess Biosyst. Eng. (2016) 1–8.
[25] J. Cheng, J. Sun, Y. Huang, J. Feng, J. Zhou, K. Cen, Dynamic microstructures and fractal characterization of cell wall disruption for microwave irradiation-assisted lipid extraction from wet microalgae, Bioresour. Technol. 150 (2013) 67–72.
[26] Y. Tan, J. Lin, Biomass production and fatty acid profile of a *Scenedesmus rubescens*-like microalga, Bioresour. Technol. 102 (21) (2011) 10131–10135.
[27] R. Praveenkumar, K. Shameera, G. Mahalakshmi, M.A. Akbarsha, N. Thajuddin, Influence of nutrient deprivations on lipid accumulation in a dominant indigenous microalga *Chlorella* sp., BUM11008: evaluation for biodiesel production, Biomass Bioenergy 37 (2012) 60–66.
[28] A.J. Klok, D.E. Martens, R.H. Wijffels, P.P. Lamers, Simultaneous growth and neutral lipid accumulation in microalgae, Bioresour. Technol. 134 (2013) 233–243.
[29] Z.Y. Liu, G.C. Wang, B.C. Zhou, Effect of iron on growth and lipid accumulation in *Chlorella vulgaris*, Bioresour. Technol. 99 (11) (2008) 4717–4722.
[30] R. Münkel, U. Schmid-Satiger, A. Werner, T. Hirth, Optimization of outdoor cultivation in flat panel airlift reactors for lipid production by *Chlorella vulgaris*, Biotechnol. Bioeng. 110 (11) (2013) 2882–2893.
[31] G. Breuer, P.P. Lamer, D.E. Martens, R.B. Daisha, R.H. Waffles, Effect of light intensity, pH, and temperature on triacylglycerol (TAG) accumulation induced by

nitrogen starvation in *Scenedesmus obliquus*, Bioresour. Technol. 143 (2013) 1–9.
[32] O.D. Clerck, M.D. Guiry, F. Leliaert, Y. Samym, H. Verbruggen, Algae taxonomy: a road to nowhere, J. Phycol. (2012) 1–11.
[33] K.L. Yeh, J.S. Chang, Effects of cultivation conditions and media composition on cell growth and lipid productivity of indigenous microalga *Chlorella vulgaris* ESP-31, Bioresour. Technol. 105 (2012) 120–127.
[34] C.H. Su, L.J. Chien, J. Gomes, Y.S. Lin, Y.K. Yu, J.S. Liou, R.J. Syu, Factors affecting lipid accumulation by *Nannochloropsis oculata* in a two-stage cultivation process, J. Appl. Phycol. 23 (5) (2011) 903–908.
[35] V. Ördög, W.A. Stirk, P. Bálint, C. Lovász, O. Pulz, J. van Staden, Lipid productivity and fatty acid composition in *Chlorella* and *Scenedesmus* strains grown in nitrogen-stressed conditions, J. Appl. Phycol. 25 (1) (2013) 233–243.
[36] C.Y. Chen, X.Q. Zhao, H.W. Yen, S.H. Ho, C.L. Cheng, D.J. Lee, F.W. Bai, J.S. Chang, Microalgae-based carbohydrates for biofuel production, Biochem. Eng. J. 78 (2013) 1–10.
[37] B. Gris, T. Morosinotto, G.M. Giacometti, A. Bertucco, E. Sforza, Cultivation of Scenedesmus obliquus in photobioreactors: effects of light intensities and light–dark cycles on growth, productivity, and biochemical composition, Appl. Biochem. Biotechnol. 172 (5) (2013) 2377–2389.
[38] Z. Li, S. Wakao, B.B. Fischer, K.K. Niyogi, Sensing and responding to excess light, Annu. Rev. Plant Biol. 60 (2009) 239–260.
[39] P.J. Nixon, F. Michoux, J. Yu, M. Boehm, J. Komenda, Recent advances in understanding the assembly and repair of photosystem II, Ann. Bot. 106 (2010) 1–16.
[40] D. Pal, I. Khozin-Goldberg, Z. Cohen, S. Boussiba, The effect of light, salinity, and nitrogen availability on lipid production by *Nannochloropsis* sp, Appl. Microbiol. Biotechnol. 90 (4) (2011) 1429–1441.
[41] D. Simionato, E. Sforza, E. Corteggiani, A. Bertucco, G.M. Giacometti, T. Morosinotto, Acclimation of *Nannochloropsis gaditana* to different illumination regimes: effects on lipids accumulation, Bioresour. Technol. 102 (2011) 6026–6032.
[42] J. Liu, C. Yuan, G. Hu, F. Li, Effects of light intensity on the growth and lipid accumulation of Microalga *Scenedesmus* sp. 11-1 under nitrogen limitation, Appl. Biochem. Biotechnol. 166 (8) (2012) 2127–2137.
[43] A.E. Solovchenko, I. Khozin-Goldberg, S. Didi-Cohen, Z. Cohen, M.N. Merzlyak, Effects of light intensity and nitrogen starvation on growth, total fatty acids and arachidonic acid in the green microalga *Parietochloris incise*, J. Appl. Phycol. 20 (3) (2008) 245–251.